PNAS
www.pnas.org

Supplementary Information for

Metabolic regulation and glucose sensitivity of cortical radial glial cells

Brian G. Rash[1], Nicola Micali[1], Anita J. Huttner[1,2], Yury M. Morozov[1], Tamas L. Horvath,[1,3,4] Pasko Rakic[1,4*]

***Author for correspondence**:

Pasko Rakic,

Duberg Professor of Neuroscience and Neurology

Kavli Institute for Neuroscience at Yale

Yale University School of Medicine, P.O Box 208100,

New Haven, CT, 06520, USA.

FAX: 203-785-3380 PHONE: 203-785-4326

E-MAIL: pasko.rakic@yale.edu

This PDF file includes:

Figs. S1 to S7
Captions for movies S1 to S13
Supplementary Methods

Other supplementary materials for this manuscript include the following:

Movies S1 to S13

www.pnas.org/cgi/doi/10.1073/pnas.1808066115

Supplementary Methods

High fat diet animals and tissue processing

All animal procedures were performed in accordance with the policies of the Yale Institutional Care and Use Committee. For *in vivo* obesity experiments, a total of 16 CD-1 dams were housed at the Yale animal facility and placed on a high fat diet (HFD; 45% fat calories) for a period of three months prior to breeding with four CD-1 males, selected for obesity and hyperglycemia (fasting blood glucose > 120 mg/dL; glucose tolerance test 337.1 ± 22.6 mg/dL, N=16), and kept on the HFD throughout pregnancy. Breeding highly obese mice is very difficult; of eight dams over 60g in weight, only one plugged over a period of three months of breeding. Noon of the day of plug detection was designated E0.5. A pulse of BrdU (50mg/kg; Sigma) was given intraperitoneally (I.P.) at E12.5. Control and experimental dams were killed at E17.5 and the brains of embryos were processed as described previously (1). Briefly, brains were dissected and immerse-fixed overnight in 4% paraformaldehyde in PBS, followed by cryoprotection in 30% sucrose and cryostat sectioning at 25 μm. Immunohistochemistry was performed as described (1). Primary antibodies and dilutions were: goat anti-Sox2 (Santa Cruz; 1:500), chicken anti-Tbr2 (Millipore; 1:500), rat anti-BrdU (Accurate Chemical; 1:400); secondary antibodies and dilutions were: donkey anti-goat/chicken/rat, 1:1000, DyLight 488/543/633 (Jackson Laboratories).

in utero electroporation (IUE)

A total of 53 timed-pregnant CD-1 mice were purchased from Charles River Laboratories for IUE experiments and housed at the Yale animal facility. Pregnant dams

were anaesthetized by ketamine/xylazine I.P. injection and IUE was performed as described previously (2). A total of 148 embryos were co-electroporated with the optogenetic sensor, pCAG-GCaMP5G (3) (Addgene), which reports changes in the concentration of cytosolic Ca^{2+}, and pCAG-BFP together, or in combination with pPAmCherry-Mito (Addgene), pmEGFP-ER-5a (Addgene), or LifeAct-mRuby (Addgene), at E14.5 and allowed to develop *in utero* for about 14 hours.

Live Slice Imaging

Dams were killed by cervical dislocation and the electroporated embryos were harvested about 14 hours post-electroporation, and the brains quickly dissected and placed into ice cold artificial cerebrospinal fluid (ACSF: 125 mM NaCl, 5 mM KCl, 1.25 mM NaH_2PO_4, 1.25 mM $MgCl_2$, 2 mM $CaCl_2$, 25 mM $NaHCO_3$, 10 mM dextrose) bubbled with 95% O_2 and 5% CO_2. The relatively short survival time ensured that the RGCs labeled through IUE did not have time to differentiate; thus, most labeled cells were RGCs with clearly visible radial fibers. Brains were embedded in 3.2% agarose (Sigma) in PBS and 300 μm slices quickly made on a Leica VT1000S vibrating microtome, and then placed in oxygenated ACSF to recover at room temperature for 20 minutes. Slices were then kept up to 24 hours in ice cold, oxygenated ACSF until imaging. Imaging at 37°C utilized a cover-glass bottom petri dish (MatTek) mounted on a heated stage with a heated ACSF delivery and aspiration system (Warner Instruments) mounted on an inverted Zeiss 510 Meta confocal microscope with a titanium sapphire 2 photon laser (Coherent). BFP Z-stacks were acquired at 780nm excitation using the 2-photon laser, while GCaMP5 movies were acquired under 488 argon laser excitation. A

LP505 emission filter was used in order to collect the maximum emitted light. Mito-mCherry images utilized 543nm excitation and an LP560 emission filter. Imaging depth was a minimum of 20 μm in order to avoid damaged cells near the slice surface. CCCP, 2,4-DNP, 2-APB (Sigma), and supplemental dextrose were dissolved in oxygenated ACSF immediately before bath application and imaging. Movies were acquired at scan rates ranging from 1Hz to 0.25Hz with 1024x1024 resolution, and slices were imaged for up to 4 hours.

Calcium Signal Detection

Image processing and Ca^{2+} signal detection was performed as previously described (1). Briefly, this was done using ImageJ (NIH, Bethesda, MD) and custom software routines written in Matlab (Mathworks, Natick, MA) (4). A motion correction algorithm implemented with the StackReg plugin was first applied to the movie to correct for small X-Y displacements within the focal plane. Cell contours corresponding to cell bodies, fibers, endfeet or other cellular regions were semi-automatically identified in the average image, *F0*, and an ROI mask created around each cellular element. ROIs were binned by user-defined anatomical regions corresponding to the VZ, SVZ/IZ, CP and MZ. Calcium signals for each ROI were defined as deviations from the average fluorescence intensity inside each ROI in each frame, *Ft*, measured as a function of time ($\Delta F/F = (Ft - F0)/F0$). Calcium events were extracted using automatic detection routines confirming events as local maxima (> 2 standard deviations of the derivative of the signal). Movie segments containing drift out of the field of focus were excluded from calcium event detection. Calcium event onsets were set as the first frame in the rising

phase of the signal. Event offsets were set as the half-amplitude decay time for each Ca^{2+} transient.

Mouse NSCs Culture and Ca^{2+} Imaging

Embryonic day (E) 11.5 embryos were isolated from pregnant C57BL/6 mice (Charles River). Dorsal cortices were collected in DMEM/F12 medium with N2 supplement, containing 25 μg/ml bovine insulin (Sigma, I6634), 100 μg/mL apotransferrin (Sigma, T2036), 20nM progesterone (Sigma, P8783), 100μM putrescine (Sigma, P5780), 30nM sodium selenite (Sigma, S5261), penicillin/streptomycin (life technology, 15140-122) and by mechanical trituration separated into single cells, as previously described (5). 1 x 10^6 cells were plated over 10 cm culture plates (Falcon 35-3003), previously coated with poly-L-ornithine (PLO) (Sigma, P3655) and fibronectin (FN) (R&D Systems, 1030FN), and incubated at 37°C, 5% O_2 and 5% CO_2 for 5 days in DMEM/F12 medium (Mediatech 16-405-CV). 10ng/mL bFGF (R&D Systems, 4114-TC) was added daily. Neural stem cells (NSCs) were lifted with HBSS (Thermo Fisher scientific, 14185052) and frozen at -80 °C. Thawed NSCs were expanded for 4 days until 80% confluence in presence of 10ng/mL FGF2, dissociated to single cells with HBSS and passaged into DMEM/F12 medium with N2 supplement and 1 ng/mL bFGF, over PLO/ fibronectin-coated 35 mm glass coverslip wells (Mat Tek, Ashland, MA), at a density of 50,000/well. bFGF was added daily. Mouse NSC cultures were labeled with Fluo4 and MitoTracker Red (Life Technologies) at a concentration of 1 μM and 200 nM, respectively, and imaged between 48-72 hr post-passage in fresh culture medium on a

Zeiss LSM 880 confocal microscope fitted with a culture chamber insert and heated stage enclosure, at 37°C with 5% O_2 and 5% CO_2.

Generation of Human Induced Pluripotent Stem Cells

Human iPSCs were generated using methods described previously (6). Briefly, fibroblast cultures were established from a small skin sample that was derived at the time of autopsy from the upper chest wall of a presumed normal 24-week old stillborn patient. Standard operating procedures and Yale institutional guidelines for the collection, handling and use of human samples were followed. Skin fibroblasts were grown according to standard conditions in DMEM supplemented with 10% FBS and antibiotics/antimycotics. After reaching 80% confluence, the cultures were passaged. To generate IPSC lines, fibroblasts were nucleofected (Amaxa system) with episomal plasmids expressing *OCT3/4, SHp53, SOX2, KLF4, LIN28, and L-MYC (Addgene)*. 24 hours after nucleofection the cell culture medium was switched to mTeSR-1 and changed daily. Round, flattened colonies appeared after approximately 2 weeks and developed into compact cultures with cobble stone morphology. Individual clones were picked manually and expanded under feeder free conditions on matrigel in mTeSR-1 medium. The cultures were passaged every 2-3 days to maintain dense cobble stone morphology. Cultures were closely monitored for signs of differentiation, and differentiating cells were removed manually. iPSC identity was confirmed when reprogrammed cells showed expression of pluripotency markers OCT4, Nanog, SOX2, TRA-1-60 and TRA-1-81.

Data Analysis

Calcium imaging data sets were analyzed using custom routines written in MATLAB (The Mathworks, Natick, MA) and in R (The R Project for Statistical Computing, http://www.r-project.org). Calcium event properties (amplitude, duration, frequency) were extracted using the event onset and offset times in the data time series for each ROI of each recording and used for population level analysis. Active ROIs were ROIs exhibiting at least one Ca^{2+} event during a recording period. Brightness plots were constructed using ImageJ to extract average brightness intensities of user-defined ovoid regions of interest. $\Delta F/F$ movies were constructed in ImageJ using custom scripts defining average X-Y image brightness and computing the difference at each time frame; results were displayed using the heatmap lookup table. Distribution means were statistically compared using an unpaired, two-tailed Student's t-tests ($p < 0.05$ was the definition of significance). Values are reported as means with the standard error of the mean (SEM).

Mitochondrial transport rates in RGC fibers were calculated by marking the start and end points of mitochondrial movement events in a movie and dividing the distance traveled by the product of the number of intervening movie frames multiplied by the frame scanning time. Kymographs were constructed in ImageJ by reslicing mitochondrial/Ca^{2+} movies along the time (Z) axis followed by a maximum intensity Z projection. Relative local Ca^{2+} levels were measured using GCaMP5 brightness within the region of dual kymograph representing stationary or motile mitochondria. Values were compared with an unpaired, two-tailed Student's t-test and reported as means. For all statistical comparisons, at least three technical replicates (separate embryos) were analyzed. Error bars represent SEM.

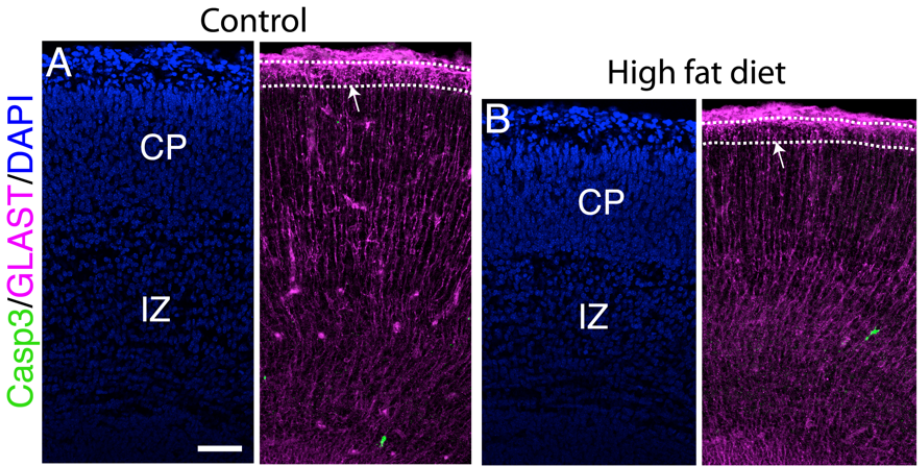

Fig. S1. High fat diet-induced obesity/hyperglycemia impairs maturation of RGC radial fibers and endfeet, without increasing cell death. Coronal sections of E17.5 CD1 cortex from embryos of control and HFD mothers. Apoptotic cells ($Casp3^{+}$) were rare in both groups (A, B), but RGC basal fibers showed disorganized and immature pial endfoot projections in the MZ (arrows; the MZ is bounded by dotted lines). Scale bar: 50 μm.

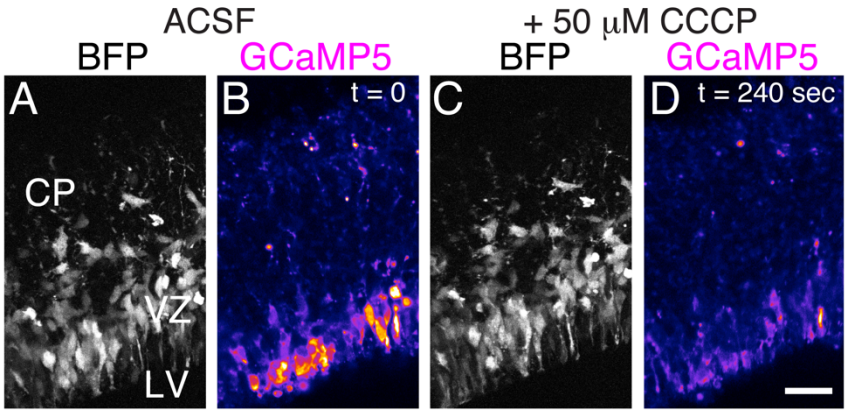

Fig. S2. Mouse brains were electroporated at E14.5 with plasmid DNA containing BFP (A, C), GCaMP5 (B, D), and Mito-mCherry (Fig. 3), and optogenetic signals recorded 14 hours later. Exposure to 50 μM CCCP reduced the brightness of GCaMP5 signals within seconds, indicating reduced cytosolic [Ca^{2+}]. Scale bar: 50 μm.

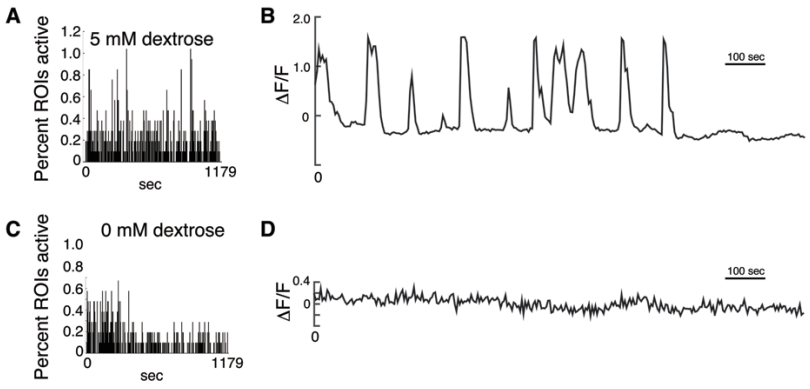

Fig. S3. Lack of Ca^{2+} activity in the absence of dextrose. At 5 mM glucose, calcium activity in RGCs is sustained at a virtually constant rate (A) for more than four hours before slices begin to show signs of degradation. An example optogenetic trace of Ca^{2+} activity in one RGC shows repetitive, almost rhythmic events 30 minutes after imaging start (B). However, application of ACSF lacking dextrose causes a rapid reduction in Ca^{2+} activity. Calcium events over 1.0 fold ΔF/F are virtually abolished within 10 minutes (C) and most RGCs show no significant Ca^{2+} activity. Exemplar trace 30 minutes after glucose withdrawal is shown in (D).

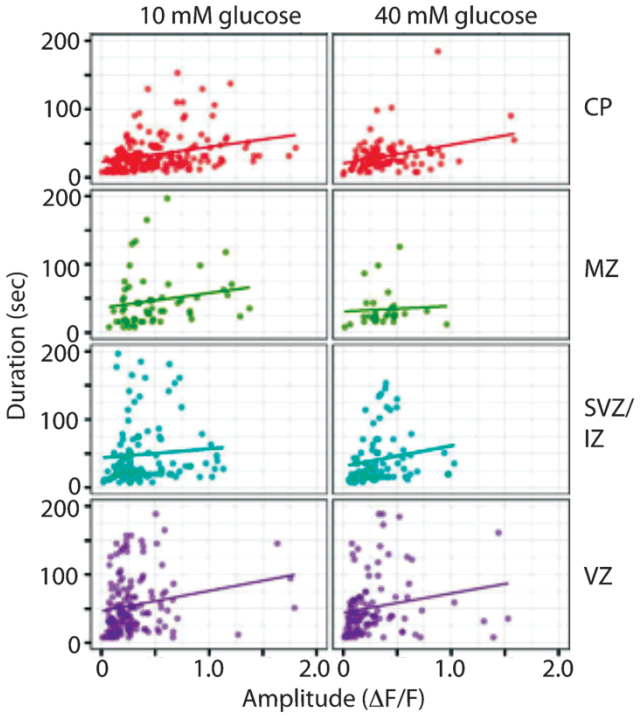

Fig. S4. Ca^{2+} activity by region in the cortical wall. Compared with euglycemia (left panels), hyperglycemia (right panels) causes reduced amplitude and duration of Ca^{2+} events in RGCs, without changes in the amp/dur relationship as indicated by the slope of the best fit lines. CP, cortical plate; MZ, marginal zone; SVZ/IZ, subventricular and intermediate zones; VZ, ventricular zone.

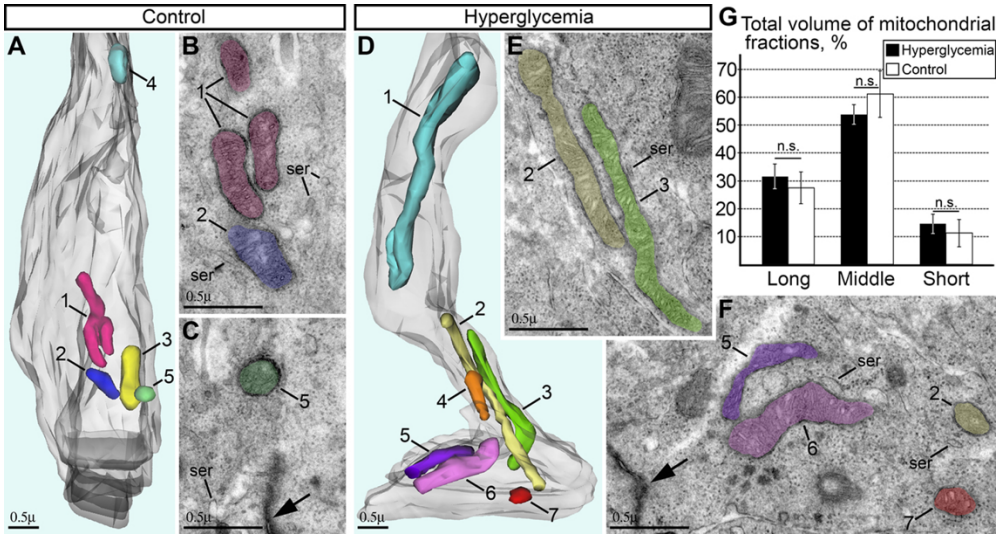

Fig. S5. Mitochondrial morphology during hyperglycemia. Electron microscopy of mitochondria in cortical RGC endfeet of E13.5 embryos after 2 hour incubation with 10 mM (euglycemia, A-C) or 40 mM (hyperglycemia, D-F) dextrose. Distinct mitochondria are color highlighted in 3D reconstructions (A and D) and corresponding electron micrographs (B, C, E and F). Mitochondria are situated in apical processes and end-feet (depicted semitransparent grey in the 3D). VZ surface is at the bottom of the 3D images (A and D). Adherent junctions between adjacent end-feet are indicated with arrows in (C) and (F). Euglycemia: mitochondrion #1 is an example of a long, branched mitochondrion; mitochondria #2-4 are middle length; mitochondrion #5 is spherical. Hyperglycemia: mitochondria #1-3 are long; mitochondria #4-6 are middle length ones; mitochondrion #7 is spherical. Notice that regardless of the length, all mitochondria show normal ultrastructure characteristic of RGCs in both euglycemic and hyperglycemic conditions. Cisterns of smooth endoplasmic reticulum (ser) are detected in all micrographs regardless of the experimental conditions. (G). Morphometric analysis of mitochondria from the embryo brain in the euglycemic (N=4) and hyperglycemic (N=4) conditions shows absence of any significant difference in the relative total volume of long, middle and short mitochondrial fractions.

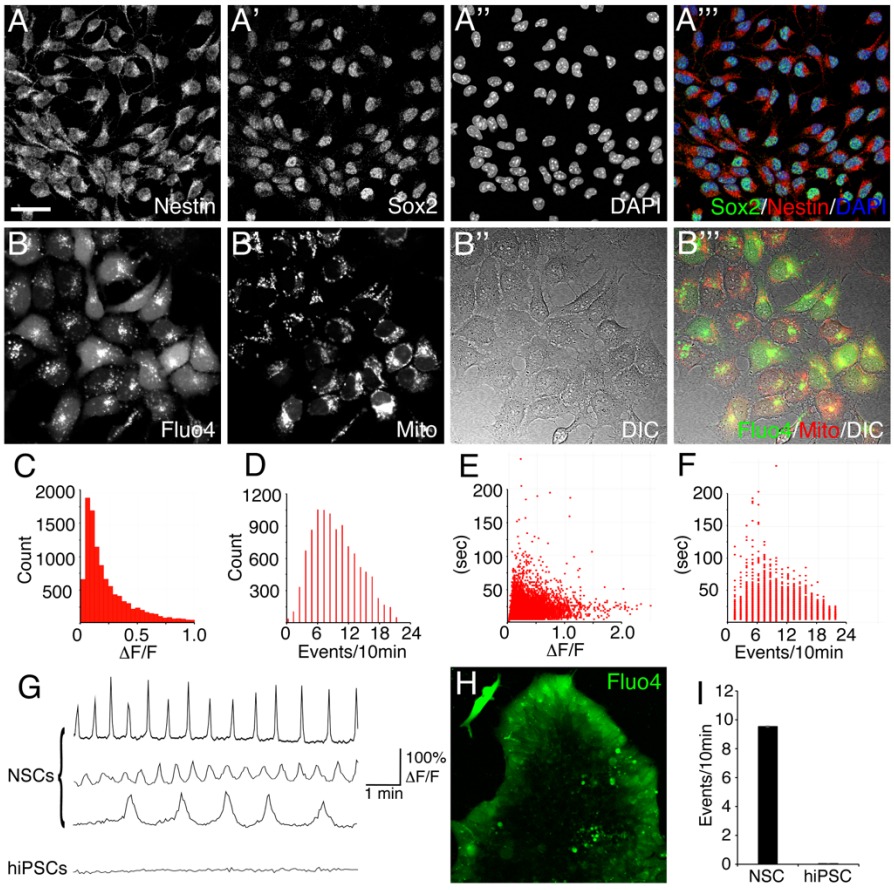

Fig. S6. Pacemaker Ca^{2+} activity in NSCs and virtual absence in hiPSCs. Cultured mouse NSCs derived from E11.5 dorsal telencephalic RGCs, 48 hours after passaging, fixed and immunostained for Nestin/Sox2 (A) or labeled with Fluo4 and Mitotracker Red (B) for live imaging (N = 4 plates). Differential interference contrast (DIC) imaging aided in determining cell-cell contacts and general cell health (B''). Calcium event properties including amplitude distribution (C), frequency distribution (D), amplitude/duration (E), and frequency/duration (F) are plotted for all events. Live recordings of Ca^{2+} fluctuations from individual NSCs utilizing the Fluo4 channel show pacemaker activity of varying frequencies (G). Human iPSCs similarly labeled with Fluo4 (H) did not show significant Ca^{2+} transient activity compared with cortical NSCs, N = 4 plates; $p < 0.0001$ (I). Scale bar: 20 μm in (A); 10 μm in (B); 30 μm in (H).

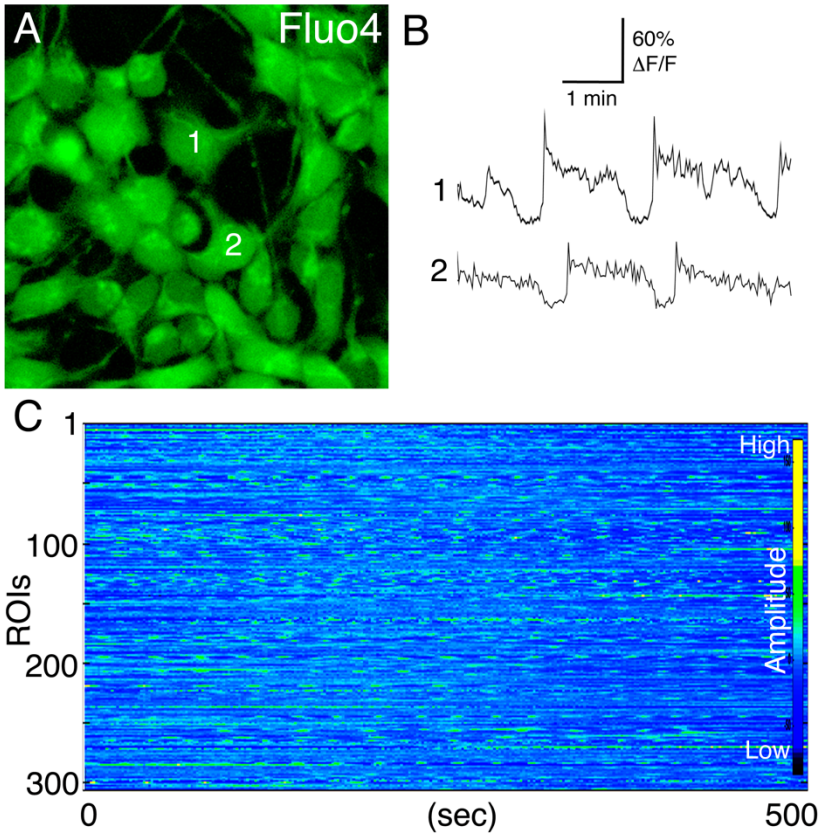

Fig. S7. Transmission of Ca^{2+} activity in NSCs. (A), Mouse cortical NSCs derived from E11.5 embryos, passaged, and 48 hr post plating labeled with Fluo4. (B), some adjacent pairs of cells showed delayed onset Ca^{2+} waveform mimicry. (C), Ca^{2+} activity recorded from over 300 ROIs in one field of view showed structured progression of events across the field, displayed as a heatmap rasterplot.

Movie S1: Calcium dynamic activity detected with GCaMP5 in RGCs at E15.5 in cortical slices.
Movie S2: Mitochondrial shuttling in RGC fibers.
Movie S3: Calcium activity is related to mitochondrial transport in RGCs in embryonic cortical slices.
Movie S4: Intracellular Ca^{2+} release appears to slow mitochondrial transport in RGC fibers.
Movie S5: Calcium dynamic activity in distal RGC fibers within the cortical plate.
Movie S6: Calcium dynamic activity in RGC fibers is quickly abolished by the inhibitor of aerobic respiration, CCCP.
Movie S7: Mitochondrial transport in RGC fibers.
Movie S8: Mitochondrial transport in RGC fibers is inhibited by CCCP.
Movie S9: Calcium activity at 10 mM glucose.
Movie S10: 40 mM glucose strongly reduces Ca^{2+} activity in RGCs.
Movie S11: Calcium activity detected with Fluo4 in cortical NSCs.
Movie S12: Mitochondrial transport is inversely correlated with Ca^{2+} events in an individual cortical NSC. NUC, nucleus.
Movie S13: In contrast with cortical NSCs, hiPSCs show only very rare Ca^{2+} transient activity (arrows).

Supplementary References

1. Rash BG, Ackman JB, & Rakic P (2016) Bidirectional radial Ca(2+) activity regulates neurogenesis and migration during early cortical column formation. *Science advances* 2(2):e1501733.
2. Rash BG, Lim HD, Breunig JJ, & Vaccarino FM (2011) FGF signaling expands embryonic cortical surface area by regulating Notch-dependent neurogenesis. *The Journal of neuroscience : the official journal of the Society for Neuroscience* 31(43):15604-15617.
3. Akerboom J, *et al*. (2012) Optimization of a GCaMP calcium indicator for neural activity imaging. *The Journal of neuroscience : the official journal of the Society for Neuroscience* 32(40):13819-13840.
4. Ackman JB, Burbridge TJ, & Crair MC (2012) Retinal waves coordinate patterned activity throughout the developing visual system. *Nature* 490(7419):219-225.
5. Adepoju A, Micali N, Ogawa K, Hoeppner DJ, & McKay RD (2014) FGF2 and insulin signaling converge to regulate cyclin D expression in multipotent neural stem cells. *Stem cells* 32(3):770-778.
6. Okita K, *et al*. (2011) A more efficient method to generate integration-free human iPS cells. *Nature methods* 8(5):409-412.